Crystal Structure and Magnetic Properties of Pyridyl-substituted Nitronyl Nitroxides

Chin-Jhan Lee*[a] (李綺縑), Ho-Hsiang Wei*[b] (魏和祥),
Gene-Hsiang Lee[c] (李錦祥) and Yu Wang[c] (王 瑜)
[a]*Deh-Yu College of Nursing and Management, Keelung, Taiwan, R.O.C.*
[b]*Department of Chemistry, Tamkang University, Tamsui, Taiwan, R.O.C.*
[c]*Instrumentation Center, College of Science, National Taiwan University, Taipei, Taiwan, R.O.C.*

X-ray crystal structure and cryomagnetic properties of three organic radicals, 2-(2-pyridyl)-4,4,5,5-tetramethyl-4,5-dihydro-1-*H*-imidazol-1-oxyl-3-N-oxide(NIT-oPy) **1**, 2-(3-pyridyl)-4,4,5,5-tetramethyl-4,5-dihydro-1-*H*-imidazol-1-oxyl-3-N-oxide(NIT-mPy) **2** and 2-(6-methyl-2-pyridyl)-4,4,5,5-tetramethyl-4,5-dihydro-1-*H*-imidazol-1-oxyl-3-N-oxide(NIT-6M-oPy) **3** were investigated. The crystal structures of compounds **1-3** show the same feature of a $P2_1/c$ space group of a monoclinic system. Two crystallographically independent molecules were found in the crystals of compounds **1-3**. The temperature dependence of magnetic susceptibility of compounds **1-3** revealed an intermolecular antiferromagnetic exchange interaction.

INTRODUCTION

The molecular design of organic materials with relevant magnetic properties is a scientific subject of increasing interest.[1-3] The members of an organic radical family, nitronyl nitroxide, NITR, have attracted much interest in this field, because of their potential antiferro- and ferromagnetic interactions.[4] Among these, nitronyl nitroxides substituted with pyridyl group and their metal complexes have been extensively studied.[5-10]

We have already reported the magneto-structural correlation for transition and non-transition metal complexes[11-14] with 2(2-, 6-methyl-2-, 3- and 4-pyridyl)-4,4,5,5-tetramethyl-4,5-dihydro-1*H*-imidazol-1-oxyl-3-N-oxide, where 2-pyridyl, 6-methyl-2-pyridyl, 3-pyridyl and 4-pyridyl substituted nitronyl nitroxide are abbreviated as NIT-oPy, NIT-6-M-oPy, NIT-mPy and NIT-oPy, respectively. Nevertheless, the crystal structures and cryomagnetic properties of these radical ligands, except NIT-pPy, have not been investigated. In the present paper, we report the syntheses, structures, and cryomagnetic properties of NIT-oPy (**1**), NIT-mPy (**2**), and NIT-6-M-oPy (**3**).

EXPERIMENTAL

Synthesis

Pyridyl-substituted nitronyl nitroxides, NIT-oPy (**1**), NIT-mPy (**2**), and NIT-6-M-oPy (**3**) are obtained by condensation of 2,3-bis(hydroxylamino)-2,3-dimethylbutane sulfate with 2-pyridinecarboxaldehyde (oPy), 3-pyridinecarboxaldehyde (mPy) and 6-methyl-2-pyridinecarboxaldehyde (6-M-oPy), respectively, followed by oxidation with lead(IV) oxide in dichloromethane at 0 °C.[15-16] Purification and recrystallization from CH_2Cl_2 gave blue crystals (m.p. = 121 °C) of **1**, blue crystals (m.p. = 112 °C) of **2** and violet-blue crystals (m.p. = 90 °C) of **3**. Anal. Found: C, 61.5; H, 6.8; N, 17.9. Calcd. for $C_{12}H_{16}N_3O_2$ **1**: C, 61.5; H, 6.8; N, 18.0%. IR (KBr): 1371 cm^{-1} ($\nu_{N\text{-}O}$). Found: C, 61.5; H, 6.8; N, 17.9. Calcd. for $C_{12}H_{16}N_3O_2$ **2**: C, 61.5; H, 6.8; N, 18.0%. IR (KBr): 1371 cm^{-1} ($\nu_{N\text{-}O}$). Found: C, 62.8; H, 7.2; N, 16.7. Calcd. for $C_{13}H_{18}N_3O_2$ **3**: C, 62.9; H, 7.3; N, 16.9%. IR (KBr): 1371 cm^{-1} ($\nu_{N\text{-}O}$).

Scheme I

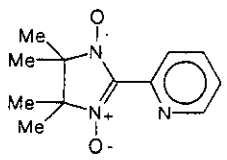

NIT-oPy 1

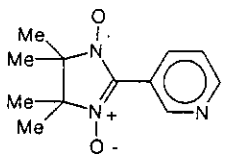

NIT-mPy 2

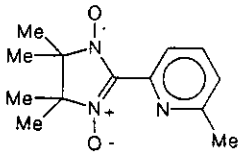

NIT-6M-oPy 3

Physical Measurements

Infrared spectra were recorded on a Bio-Rad FTS40 FTIR spectrophotometer as KBr pellets in the 400-4000 cm^{-1} region. X-band EPR spectra at 300 K for the compounds in benzene solution were recorded on a Bruker ESC-106 spectrometer. The temperature dependence of the magnetic susceptibility of the polycrystalline samples were measured between 4 and 300 K at field 1 T using a Quantum Design Model MPMS computer-controlled SQUID magnetometer. Diamagnetic corrections were made using Pascal's constants.[17]

X-Ray Crystallography

Well-shaped crystals of NIT-oPy **1**, NIT-mPy **2** and NIT-6M-oPy **3**, obtained as described above, were suitable for X-ray analysis. The data were collected at 25 °C with an Enraf-Nonius CAD4 diffractometer using graphite-monochromated Mo K_α radiation. The detailed crystallographic data for the complexes are listed in Table 1. The complete bond distances and angles, atomic coordinates, and thermal parameters are given as supplementary material.

RESULTS AND DISCUSSION

Crystal Structures of Compounds 1-3

The results of the X-ray crystal structures analysis with the atom-numbering scheme in compounds **1-3** are reproduced in Figs. 1-3, respectively. The selected bond distances and angles are given in Table 2-4. The crystal structures show the same feature of a $P2_1/c$ space group of a monoclinic system. Two crystallographically independent molecules were found in the crystals of compounds **1-3**.

As shown in Fig. 1, in compound **1**, the fragments O(1)-N(1)-C(6)-N(2)-O(2) [N(1)-O(1) 1.276(4), N(2)-O(2) 1.281(4) Å] and O(1)′-N(1)′-C(6)′-N(2)′-O(2)′ [N(1)′-O(1)′ 1.281(4), N(2)′-O(2)′ 1.280(4) Å] are nearly planar but form the dihedral angles of 50.1(1) and 61.48(14)° with planes of the pyridyl rings, respectively.

The structure of compound **2** consists of two crystallographically independent units. The O(1)-N(1)-C(6)-N(2)-O(2) [N(1)-O(1) 1.270(5), N(2)-O(2) 1.275(5) Å] and O(1)′-N(1)′-C(6)′-N(2)′-O(2)′ [N(1)′-O(1)′ 1.275(5), N(2)′-O(2)′ 1.270(5) Å] moieties are as expected nearly planar,

Table 1. Crystallographic Data

Compounds	NIT-oPy	NIT-mPy	NIT-6M-oPy
Formula	$C_{12}H_{16}N_3O_2$	$C_{12}H_{16}N_3O_2$	$C_{13}H_{18}N_3O_2$
Formula weight	234.28	234.28	248.30
Space group	Monclinic $P2_1/c$	Monoclinic $P2_1/c$	Monclinic $P2_1/c$
a (Å)	6.190(3)	6.1729(9)	6.3698(7)
b (Å)	30.283(9)	30.292(4)	26.753(15)
c (Å)	13.116(4)	13.0640(13)	15.610(7)
β (°)	100.74(3)	100.959(11)	95.729(18)
V ($Å^3$)	2415.7(14)	2398.2(5)	2646.7(19)
Z	8	8	8
D_{calc} (g cm^{-3})	1.288	1.298	1.246
λ (Mo-K_α)(Å)	1.5418	0.7107	0.7107
F(000)	1003	1000	1064
Unit cell detection, No; (2θ range)	25; (33.52-52.02)	25; (12.70-22.14)	25; (14.50-28.06)
Scan type	θ-2θ	θ-2θ	θ-2θ
2θ scan width (°)	2(0.75 + 0.15 tanθ)	2(0.60 + 0.35 tanθ)	2(0.65 + 0.35 tanθ)
2θ range (°)	140.0	45.0	45.0
μ (Mo-K_α) (cm^{-1})	6.970	0.874	0.810
Crystal size (mm)	0.50 × 0.50 × 0.60	0.10 × 0.25 × 0.40	0.30 × 0.40 × 0.40
Temperature (K)	298	298	298
No. of unique reflection	4455	3135	3452
No. of obs. reflection [I > 2θ(I)]	3799	1575	2272
R, R_w*	0.074, 0.074	0.041, 0.040	0.045, 0.047
Computer program	NRCVAX**	NRCVAX	NRCVAX

* $R = \Sigma(|F_o| - |F_c|)/\Sigma|F_o|$, $R_w = [\Sigma w(|F_o| - |F_c|)^2/\Sigma(|F_o|)^2]^{1/2}$

** NRCVAX: Gabe, E. J.; Le-Page, Y.; Cherland, J. P.; Lee, F.; White, P. S. *J. Appl. Cryst.* **1989**, *22*, 384.

Table 2. Selected Bond Distances (Å) and Angles (°) for **1**

Distances			
N(1)-O(1)	1.276(4)	N(1)′-O(1)′	1.281(4)
N(2)-O(2)	1.281(4)	N(2)′-O(2)′	1.280(4)
N(1)-C(6)	1.343(4)	N(1)′-C(6)′	1.337(4)
N(2)-C(6)	1.356(5)	N(2)′-C(6)′	1.348(5)
N(3)-C(5)	1.334(5)	N(3)′-C(5)′	1.327(5)
N(3)-C(1)	1.334(5)	N(3)′-C(1)′	1.347(5)
C(5)-C(6)	1.469(5)	C(5)′-C(6)′	1.476(5)
Angles			
O(1)-N(1)-C(6)	125.4(3)	O(1)′-N(1)′-C(6)′	125.6(3)
O(1)-N(1)-C(7)	122.0(3)	O(1)′-N(1)′-C(7)′	122.0(3)
O(2)-N(2)-C(6)	126.0(3)	O(2)′-N(2)′-C(6)′	125.4(3)
N(1)-C(6)-C(5)	126.2(3)	N(1)′-C(6)′-C(5)′	123.8(3)
N(2)-C(6)-C(5)	124.8(3)	N(2)′-C(6)′-C(5)′	126.7(3)
N(3)-C(5)-C(6)	116.5(3)	N(3)′-C(5)′-C(6)′	116.1(3)
C(4)-C(5)-C(6)	119.9(3)	C(4)′-C(5)′-C(6)′	119.9(3)

but form the dihedral angles of 39.8(2) and 56.8(2)° with the plane of pyridyl rings, respectively.

The structure of compound **3** also consists of two crystallographically independent units. The O(1)-N(1)-C(7)-N(2)-O(2) [N(1)-O(1) 1.282(4), N(2)-O(2) 1.277(4) Å] and O(3)-N(4)-C(20)-N(5)-O(4) [N(4)-O(3) 1.284(4), N(5)-O(4) 1.275(4) Å] moieties are nearly planar, but form the dihedral angles of 57.3(1) and 67.3(1)° with the pyridyl rings, respectively. The shortest contact distance of C(13)···O(3) between two different NIT-6M-oPy radicals is 3.399(5) Å, which can be considered as weak hydrogen bonding interaction between the hydrogen atom of $C(13)H_3$ and the oxygen atom of N(4)-O(3) groups.

EPR Spectra and Magnetic Properties

The EPR (at 9.80 GHz) spectra at 300 K of compounds **1**-**3** in benzene solution show five similar major lines in the ratio 1:2:3:2:1 as expected for coupling with two identical

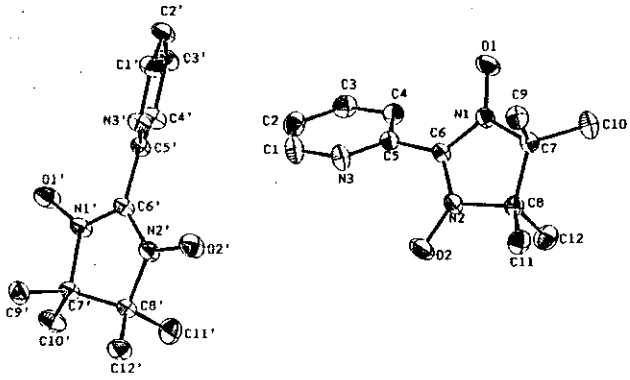

Fig. 1. Structural representation of NIT-oPy (**1**) with atom-labelling scheme (30% probability thermal ellipsoids).

Table 3. Selected Bond Distances (Å) and Angles (°) for **2**

Distances			
N(1)-O(1)	1.270(5)	N(1)′-O(1)′	1.275(5)
N(2)-O(2)	1.270(5)	N(2)′-O(2)′	1.270(5)
N(1)-C(6)	1.354(5)	N(1)′-C(6)′	1.345(6)
N(2)-C(6)	1.343(5)	N(2)′-C(6)′	1.345(5)
C(4)-C(6)	1.450(6)	C(4)′-C(6)′	1.465(6)
N(3)-C(5)	1.332(6)	N(3)′-C(5)′	1.328(6)
N(3)-C(1)	1.330(7)	N(3)′-C(1)′	1.320(7)
Angles			
O(1)-N(1)-C(6)	125.5(3)	O(1)′-N(1)′-C(6)′	126.0(3)
O(2)-N(2)-C(6)	125.7(4)	O(2)′-N(2)′-C(6)′	125.5(4)
O(1)-N(1)-C(8)	122.2(3)	O(1)′-N(1)′-C(8)′	121.6(3)
N(1)-C(6)-N(2)	108.5(4)	N(1)′-C(6)′-N(2)′	109.4(4)
N(1)-C(6)-C(4)	126.5(4)	N(1)′-C(6)′-C(4)′	124.2(4)
N(2)-C(6)-C(4)	125.0(4)	N(2)′-C(6)′-C(4)′	126.4(4)
C(6)-C(4)-C(5)	120.8(4)	C(6)′-C(4)′-C(5)′	120.2(4)
C(6)-C(4)-C(3)	121.5(4)	C(6)′-C(4)′-C(3)′	121.3(4)
C(1)-N(3)-C(5)	115.8(4)	C(1)′-N(3)′-C(5)′	116.8(4)

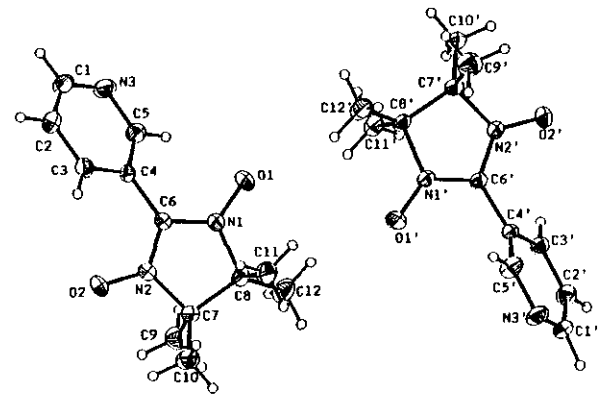

Fig. 2. Structural representation of NIT-mPy (**2**) with atom-labelling scheme (30% probability thermal ellipsoids).

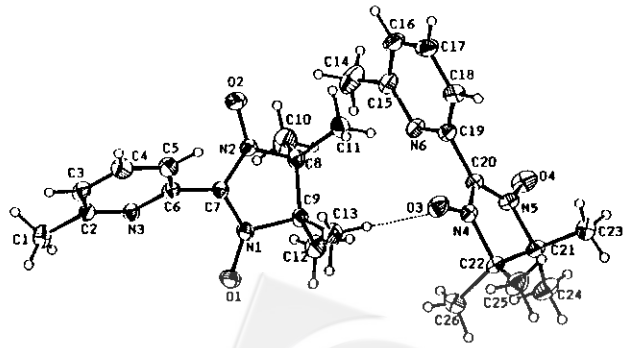

Fig. 3. Structural representation of NIT-6-M-oPy (**3**) with atom-labelling scheme (30% probability thermal ellipsoids). Weak hydrogen bond between nitoxide oxygen, O(3), and hydrogen atom of $C(13)H_3$ is represented by dashed line.

Table 4. Selected Bond Distances (Å) and Angles (°) for **3**

Distances			
N(1)-O(1)	1.282(4)	N(4)-O(3)	1.284(4)
N(2)-O(2)	1.277(4)	N(5)-O(4)	1.275(4)
N(1)-C(7)	1.338(4)	N(4)-C(20)	1.329(4)
N(2)-C(7)	1.338(4)	N(5)-C(20)	1.343(5)
N(2)-C(8)	1.512(4)	N(5)-C(21)	1.515(4)
N(1)-C(9)	1.511(4)	N(4)-C(22)	1.504(4)
C(6)-C(7)	1.470(5)	C(19)-C(20)	1.474(4)
N(3)-C(6)	1.339(5)	C(19)-N(6)	1.332(5)
N(3)-C(2)	1.336(4)	N(6)-C(15)	1.341(4)
Angles			
O(1)-N(1)-C(7)	126.1(3)	O(3)-N(4)-C(20)	125.7(3)
O(2)-N(2)-C(7)	126.0(3)	O(4)-N(5)-C(20)	126.6(3)
O(1)-N(1)-C(9)	121.59(25)	O(3)-N(4)-C(22)	121.9(3)
O(2)-N(2)-C(8)	121.5(3)	O(4)-N(5)-C(21)	121.6(3)
N(1)-C(7)-N(2)	109.6(3)	N(4)-C(20)-N(5)	109.8(3)
N(1)-C(7)-C(6)	126.3(3)	N(4)-C(20)-C(19)	123.6(3)
N(2)-C(7)-C(6)	123.9(3)	N(5)-C(20)-C(19)	126.7(3)
N(3)-C(6)-C(7)	117.6(3)	N(6)-C(19)-C(20)	116.3(3)
C(5)-C(6)-C(7)	118.3(3)	C(18)-C(19)-C(20)	119.3(3)

nitrogens of N-O groups in the radicals. The g values are at 2.01 in all radicals, but the nitrogen hyperfine coupling constants a^N for **1**, **2**, and **3** are at 7.25, 8.25, and 7.80 G, respectively.

The $1/\chi_m$ and χ_mT vs T of **1-3** are shown in Figs. 4-6, respectively, where χ_m, $1/\chi_m$ and χ_mT are plotted as a function of temperature. The temperature dependence of $1/\chi_m$ and χ_mT of compounds **1-2** follow the Curie-Weiss law in the whole temperature range between 4 and 300 K. The Curie-Weiss law (equation 1) was used to fit the magnetic data.

$$\chi_m = Ng^2\mu_B{}^2S(S+1)/3k(T-\theta) \quad (1)$$

The values obtained for θ in this manner are -0.39 and -1.27 K for **1** and **2**, respectively.

Fig. 6 displays the plots of χ_m (per radical) and χ_mT vs T in the range 4-300 K for compound **3**. The χ_mT (per radical) value, decreases from 0.39 $cm^3K\ mol^{-1}$ at 300 K with decreasing temperature down to the value of 0.23 $cm^3K\ mol^{-1}$ at 4 K, indicating the presence of antiferromagnetic ex-

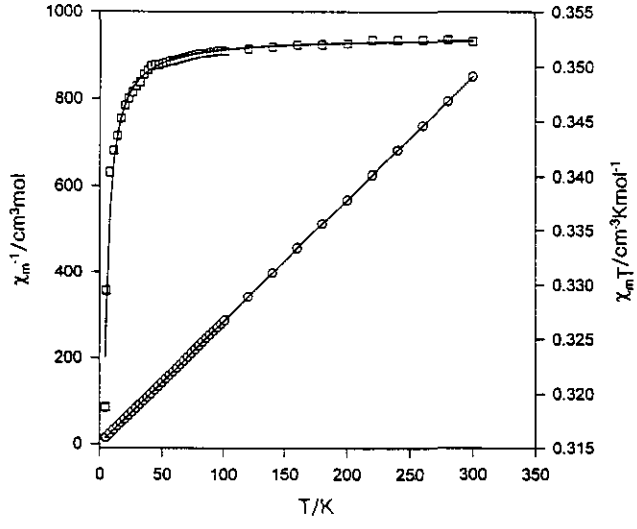

Fig. 4. Thermal variation of the molar magnetic susceptibility for per NIT-oPy (**1**), in the forms of $1/\chi_m$ (o) and χ_mT (□) *versus* T. The solid lines are the best theoretical fits (see text).

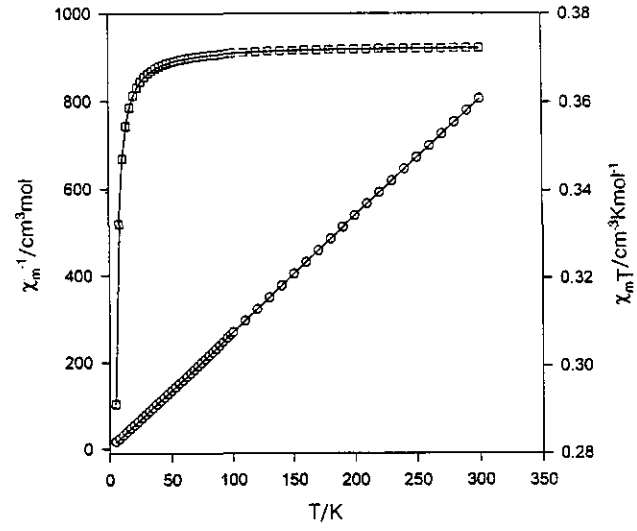

Fig. 5. Thermal variation of the molar magnetic susceptibility for per NIT-mPy (**2**), in the forms of $1/\chi_m$ (o) and χ_mT (□) *versus* T. The solid lines are the best theoretical fits (see text).

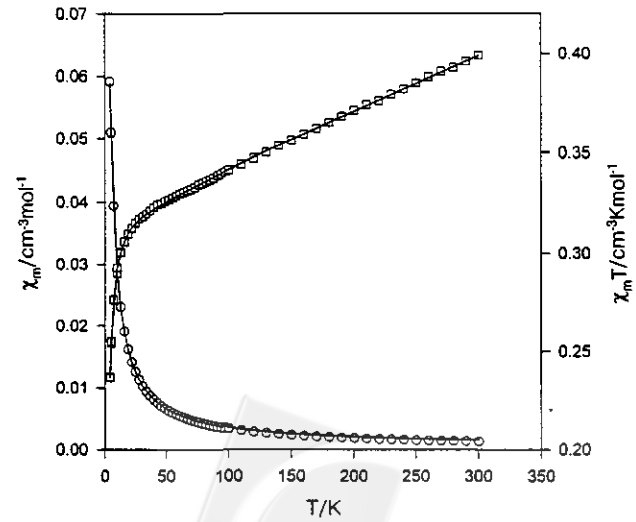

Fig. 6. Thermal variation of the molar magnetic susceptibility for per NIT-6M-oPy (**3**) in the forms of χ_m (o) and χ_mT (□) *versus* T. The solid lines are the best theoretical fits (see text).

change interaction. According to the crystal structure for this compound, possible pathways for the exchange involve the weak hydrogen bonding of C(13)-H···O(3) between two neighbour NIT-6-M-oPy radicals. Accordingly, we examined fits of the susceptibilities to the dinuclear Heisenberg model for the $S_1 = S_2 = 1/2$ system. The theoretical expression for the χ_m (per molecule) of a dinuclear spin system of S = 1/2 is given by equation 2,[18] where θ is the Weiss constant which correlates to the intermolecular interaction, N_α is temperature-independent susceptibility, and N, μ_B and k have their usual meanings.

$$\chi_m = [N\mu_B^2 g^2/3k(T - \theta)]\,[1 + (1/3)\exp(-2J/kT)]^{-1} + N_\alpha \quad (2)$$

The solid curve for **3** in Fig. 6 represents the best fit of the experimental data obtained with $J = -3.44\ cm^{-1}$, θ = -2.95 K, g = 2.0, and $N_\alpha = 27 \times 10^{-5}\ cm^3mol$. The discrepancy, $R = 2.0 \times 10^{-5}$, is defined as $R = (\chi_{obs} - \chi_{calc})^2/(\Sigma\chi_{obs})^2$.

ACKNOWLEDGEMENTS

This research was supported by a grant (NCS86-2113-M-32-005) from the National Science Council of Taiwan.

Received December 31, 1997.

Key Words

Molecular magnetism; Crystal structure; Organic radicals; Nitronyl nitroxides.

REFERENCES

1. Miller, J. S.; Epstein, A. J.; Reiff, W. M. *Chem. Rev.* **1988**, *88*, 201.
2. Gatteschi, D.; Kahn, O.; Miller, J. S.; Palacio, F. eds., *Magnetic Molecular Materials*, NATOASI Series E, Kluwer, Dorecht, 1991.
3. Iwamura, H.; Miller, J. S. Eds., *Mol. Cryst. Liq. Cryst.* **1993**, *232*, 233.
4. Hernandez, E.; Mas, M.; Molins, E.; Rovira, C.; Vecians, J. *Angew. Chem. Int. Ed. Engl.* **1993**, *32*, 882, and references cited therein.
5. Awaga, K.; Inabe, T.; Maruyama, Y. *Synthetic Metals.* **1993**, *55-57*, 3311, *Chem. Phys. Lett.* **1992**, *190*, 349.
6. Okuno, T.; Otsuka, T.; Awaga, K. *J. Chem. Soc., Chem. Commun.* **1995**, 827.
7. Panthou, F. L.; Belorizky, e.; Calemczuk, R.; Luneau, D.; Marcenat, C.; Ressouche, E.; Turek, P.; Rey, P. *J. Am. Chem. Soc.* **1995**, *117*, 11247.
8. Caneschi, A.; Ferraro, F.; Gatteschi, D.; Rey, P.; Sessoli, R. (a) *Inorg. Chem.* **1990**, *29*, 1756. (b) *ibid.* **1990**, *29*, 4217. (c) *ibid.* **1991**, *30*, 3162.
9. Benelli, C.; Caseschi, G,; Gatteschi, D.; Pardi, L. *Inorg. Chem.* **1992**, *31*, 741.
10. Luneau, D.; Risoan, G.; Rey, P.; Grand, A.; Caseschi, A.; Gatteschi, D.; Laugier, J. *Inorg. Chem.* **1993**, *32*, 5616.
11. Wei, H. H.; Wong, H. Y.; Lee, G. H.; Wang, Yu. *J. Chin. Chem. Soc.* (*Taipei*). **1996**, *43*, 253.
12. Huang, C. F.; Wei, H. H. *J. Chin. Chem. Soc.* (*Taipei*) **1997**, *44*, 439.
13. Huang, C. F.; Wei, H. H.; Lee, G. H.; Wang, Yu. *Inorg. Chim. Acta.* **1998** (in press).
14. Lee, C. J.; Huang, C. F.; Wei, H. H.; Liu, Y. H.; Lee, G. H.; Wang, Yu. *J. Chem. Soc., Dalton Trans.* **1998**, 171.
15. Lamchen, M.; Mittag, T. W. *J. Chem. Soc.*(c) **1966**, 2300.
16. Ullman, E. F.; Call, L.; Osiecki, J. H. *J. Org. Chem.* **1970**, *35*, 3623.
17. Kahn, O. *Molecular Magnetism.* VCH.; New York, **1993**, p. 3.
18. Bleaney, B.; Bowers, K. D. *Proc. R. Soc. London, Ser. A.* **1952**, *214*, 4519.